Perturbative QCD predictions for the decay $B_s^0 \to SS(a_0(980), f_0(980), f_0(500))$

Ze-Rui Liang[*] and Xian-Qiao Yu[†]

School of Physical Science and Technology, Southwest University, Chongqing 400715, China

(Received 20 March 2019; accepted 13 October 2020; published 4 December 2020)

In this work, we calculate the branching ratios and CP violations of the $B_s^0 \to a_0(980)a_0(980)$ decay modes with both charged and neutral $a_0(980)$ mesons and $B_s^0 \to f_0(980)(f_0(500))f_0(980)(f_0(500))$ for the first time in the pQCD approach. Considering the recent observation of the BESIII collaboration that provide a direct information about the constituent two-quark components in the corresponding $a_0(980)$ wave functions, we regard the scalar mesons $a_0(980)$, $f_0(980)$, and $f_0(500)$ as the $q\bar{q}$ quark component in our present work, and then make predictions of these decay modes. The branching ratios of our calculations are at the order of the $10^{-4} \sim 10^{-6}$ when we consider the mixing scheme. We also calculate the CP violation parameters of these decay modes. The relatively large branching ratios make it easily to be tested by the running LHC-b experiments, and it can help us to understand both the inner properties and the QCD behavior of the scalar meson.

DOI: 10.1103/PhysRevD.102.116007

I. INTRODUCTION

Since the first scalar meson $f_0(980)$ was observed by the Belle collaboration in the charged decay mode $B^\pm \to K^\pm f_0(980) \to K^\pm \pi^\mp \pi^\pm$ [1], and afterwards confirmed by *BABAR* [2], a lot of other scalar mesons have been discovered in the experiment successively. The scalar mesons, especially for the $a_0(980)$ and $f_0(980)$, which are important for understanding the chiral symmetry and confinement in the low-energy region, are one of the key problems in the nonperturbative QCD [3]. However, the inner structure of scalar mesons is still a contradiction in both the theoretical and experimental side, and many works have been done about scalar mesons in order to solve this problem [4–16]. In Ref. [3], the authors listed many evidences that sustain the four-quark model of the light scalar mesons based on a series of experimental data. In Ref. [17], the predicted result of $B \to a_0(980)K$ was 2 times difference from the experimental result, and the author conclude that $a_0(980)$ cannot be interpreted as $q\bar{q}$. In Ref. [18], the authors showed that the production of the S^* and δ and of low-mass $K\bar{K}$ pairs have properties of the $K\bar{K}$ molecules. Moreover, the scalar meson are identified as the quark-antiquark gluon hybrid. Nevertheless, these interpretations of the scalar mesons make theoretical calculations difficult, apart from the ordinary $q\bar{q}$ model.

In the theoretical side, there are two interpretations about light scalar mesons below 2 GeV in Review of Particle Physics [19], the scalars below 1 GeV, including $f_0(500)$, $K^*(700)$, $f_0(980)$, and $a_0(980)$, form a $SU(3)$ flavor nonet, and $f_0(1370)$, $a_0(1450)$, $K^*(1430)$, and $f_0(1500)$ (or $f_0(1700)$) that above 1 GeV form another $SU(3)$ flavor nonet. In order to describe the structure of these light scalar mesons, the authors of Ref. [8] presented two scenarios to clarify the scalar mesons:

(1) Scenario 1, the light scalar mesons, which involved in the first $SU(3)$ flavor nonet, are usually regarded as the lowest-lying $q\bar{q}$ states, and the other nonet as the relevant first excited states. In the ordinary diquark model, the quark components of $a_0(980)$ and $f_0(980, 500)$ are

$$a_0^+(980) = u\bar{d}, \qquad a_0^-(980) = \bar{u}d,$$
$$a_0^0(980) = \frac{1}{\sqrt{2}}(u\bar{u} - d\bar{d}), \qquad f_0(980) = s\bar{s},$$
$$f_0(500) = \frac{1}{\sqrt{2}}(u\bar{u} + d\bar{d}), \tag{1}$$

(2) Scenario 2, the scalar mesons in the second nonet are regarded as the ground states ($q\bar{q}$), and scalar mesons with mass between 2.0–2.3 GeV are first excited states. This scenario indicates that the scalars below or near 1 GeV are four-quark bound states, while other scalars consist of $q\bar{q}$ in scenario 1. So the quark components of $a_0(980)$ and $f_0(980, 500)$ are

[*]liangzr@email.swu.edu.cn
[†]yuxq@swu.edu.cn

$$
\begin{aligned}
a_0^+(980) &= u\bar{d}s\bar{s}, \qquad a_0^-(980) = \bar{u}d\bar{s}s,\\
a_0^0(980) &= \frac{1}{\sqrt{2}}(u\bar{u} - d\bar{d})s\bar{s},\\
f_0(980) &= \frac{1}{\sqrt{2}}(u\bar{u} + d\bar{d})s\bar{s}, \qquad f_0(500) = ud\bar{u}\bar{d}.
\end{aligned} \tag{2}
$$

Recently, the BESIII collaboration declare that the first measurement of D mesons semileptonic decay $D^0 \to a_0^-(980)e^+\nu_e$ and the existing evidence of $D^+ \to a_0^0(980)e^+\nu_e$ [20], which would provide useful information on revealing the mysterious nature of the scalar mesons. And in Ref. [21], BESIII declare the $a_0^0(980) - f_0(980)$ mixing in the $J/\psi \to \phi f_0(980) \to \phi a_0^0(980) \to \phi\eta\pi^0$ and $\chi_{c1} \to a_0^0(980)\pi^0 \to f_0(980)\pi^0 \to \pi^+\pi^-\pi^0$ decay modes, which is the first observation of $a_0^0(980) - f_0(980)$ mixing in experiment. In our work, we treat the scalar mesons $a_0(980)$, $f_0(980)$ as the component of $q\bar{q}$ in scenario 1, and make the theoretical calculations within the perturbative QCD approach. For $f_0(980)$, there exist a mixing with the $f_0(500)$ in the SU(3) nonet, and in this work, we also take the mixing effect into account to make more reliable results. Motivated by the uncertain inner structure of the scalar mesons and very few works about the $B \to SS$ decays (S denote the scalar mesons) to be studied in these general factorization approaches, we explore the branching ratios and CP-violating asymmetries of decay modes $\bar{B}_s^0 \to a_0(980)a_0(980)$ and $\bar{B}_s^0 \to f_0(980,500)f_0(980,500)$[1] in perturbative QCD approach within the traditional two-quark model for the first time. Because the LHC-b collaboration are collecting more and more B mesons decays data, so we believe that our results can be testified by the experiment in the near future time.

This article is organized roughly in this order: in Sec. II, we give a theoretical framework of the pQCD, list the wave functions that we need in the calculations, and also the perturbative calculations; in Sec. III, we make numerical calculations and some discussions for the results that we get; and at last, we summary our work in the final section. Some formulas what we used in our calculation are collected in the Appendix.

II. THE THEORETICAL FRAMEWORK AND PERTURBATIVE CALCULATION

The pQCD approach have been widely applied to calculate the hadronic matrix elements in the B mesons decay modes, it is based on the k_T factorization. The divergence of the endpoint singularity can be safely avoided by preserving the transverse momenta k_T in the valence quark, and the only input parameters are the wave functions of the involved mesons in this method. Then the transition form factors and the different contributions, whose may contain the spectator and annihilation diagrams, are all calculated in this framework.

A. Wave functions and distribution amplitudes

In kinematics aspects, we adopt the light-cone coordinate system in our calculation. Assuming the B_s^0 meson to be rest in the system, we can describe the momenta of the mesons in light-cone coordinate system, where the momenta are expressed in the form of (p^+, p^-, p_T) with the definition $p^\pm = \frac{p_0 \pm p_3}{\sqrt{2}}$ and $p_T = (p_1, p_2)$.

In our calculation, the wave function of the hadron B_s^0 can be found in Refs. [22–24]

$$
\Phi_{B_s^0} = \frac{i}{\sqrt{2N_c}}(\not{p}_B + m_{B_s})\gamma_5\phi_{B_s}(x_1, b_1), \tag{3}
$$

where the distribution amplitude(DA) $\phi_{B_s}(x_1, b_1)$ of B_s^0 meson is written as mostly used form, which is

$$
\phi_{B_s}(x_1, b_1) = N_B x_1{}^2(1-x_1)^2 \exp\left[-\frac{m_{B_s}^2 x_1{}^2}{2\omega_{B_s}^2} - \frac{1}{2}(\omega_{B_s} b_1)^2\right], \tag{4}
$$

the normalization factor $N_B = 62.8021$ can be calculated by the normalization relation $\int_0^1 dx\phi_{B_s}(x_1, b_1 = 0) = f_{B_s}/(2\sqrt{2N_c})$ with $N_c = 3$ is the color number and decay constant $f_{B_s} = 227.2 \pm 3.4$ MeV. Here, we choose shape parameter $\omega_{B_s} = 0.50 \pm 0.05$ GeV [25].

For the scalar meson $a_0(980)$ and $f_0(980)$, the wave function can be read as [8,15]:

$$
\Phi_S(x) = \frac{1}{2\sqrt{2N_c}}[\not{p}\phi_S(x) + m_S\phi_S^S(x) + m_S(\not{n}\not{v} - 1)\phi_S^T(x)], \tag{5}
$$

where x denotes the momentum fraction of the meson, and $n = (1, 0, 0_T)$, $v = (0, 1, 0_T)$ are lightlike dimensionless vectors.

ϕ_S is the leading-twist distribution amplitude, the explicit form of which is expanded by the Gegenbauer polynomials [8,15]:

$$
\phi_S(x, \mu) = \frac{3}{\sqrt{2N_c}}x(1-x)\{f_S(\mu) + \bar{f}_S(\mu)\sum_{m=1,3}^{\infty} B_m(\mu)C_m^{3/2}(2x-1)\}, \tag{6}
$$

[1] $a_0(980)$, $f_0(980)$, and $f_0(500)$ will be respectively abbreviated as a_0, f_0, and σ in the last part.

and for the twist-3 DAs ϕ_S^S and ϕ_S^T, we adopt the asymptotic forms in our calculation,

$$\phi_S^S(x,\mu) = \frac{1}{2\sqrt{2N_c}}\bar{f}_S(\mu), \tag{7}$$

$$\phi_S^T(x,\mu) = \frac{1}{2\sqrt{2N_c}}\bar{f}_S(\mu)(1-2x), \tag{8}$$

where f_S and $\bar{f}_S$ are the vector and scalar decay constants of the scalar mesons a_0 and f_0 respectively, B_m is Gegenbauer moment and $C_m^{3/2}(2x-1)$ in DA of ϕ_S is Gegenbauer polynomials, these parameters are scale-dependent. A lot of calculations have been carried out about the light scalar mesons in various model [26–28]. In this article, we adopt the value for decay constants and Gegenbauer moments in the DAs of the a_0 and f_0 as listed follow, which were calculated in QCD sum rules at the scale $\mu = 1$ GeV [8,15]:

$$\begin{aligned} &\bar{f}_{a_0} = 0.365 \pm 0.020 \text{ GeV}, \qquad B_1 = -0.93 \pm 0.10, \qquad B_3 = 0.14 \pm 0.08; \\ &\bar{f}_S = \bar{f}_{f_0}^n = \bar{f}_{f_0}^s = 0.370 \pm 0.020 \text{ GeV}, \qquad B_1^n = -0.78 \pm 0.08, \qquad B_3^n = 0.02 \pm 0.07, \\ &B_{1,3}^s = 0.8 B_{1,3}^n. \end{aligned} \tag{9}$$

The two decay constants $\bar{f}_{f_0}^n$ and $\bar{f}_{f_0}^s$ used in our calculations have been defined in the framework of the QCD sum rule method, here we choose the same value of these two constants and the reasons have been discussed in the Ref. [8]. It is noticeable that only the odd Gegenbauer moments are taken into account due to the conservation of vector current or charge conjugation invariance. And we also pay attention to only the Gegenbauer moments B_1 and B_3 because the higher order Gegenbauer moments make tiny contributions and can be ignored safely.

The vector and scalar decay constants satisfy the relationship

$$\bar{f}_S(\mu) = \mu_S f_S(\mu) \tag{10}$$

with

$$\mu_S = \frac{m_S}{m_1(\mu) - m_2(\mu)}, \tag{11}$$

and m_S is the mass of the scalar meson and m_1 and m_2 are the running current quark masses in the scalar meson. From the above relationship, it is clear to see that the vector decay constant is proportional to the mass difference between the m_1 and m_2 quark, the mass difference is so small after considering the $SU(3)$ symmetry breaking that would heavily suppress the vector decay constant, which lead to the vector decay constants of the scalar mesons are very small and can be negligible. Likewise, for the same reason that only the odd Gegenbauer momentums are considered, the neutral scalar mesons cannot be produced by the vector current, so in this work we adopt the vector constant $f_S = 0$.

And the normalization relationship of the twist-2 and twist-3 DAs are

$$\begin{aligned} &\int_0^1 dx \phi_S(x) = \int_0^1 dx \phi_S^T(x) = 0, \\ &\int_0^1 dx \phi_S^S(x) = \frac{\bar{f}_S}{2\sqrt{2N_c}}. \end{aligned} \tag{12}$$

For the scalar meson $f_0 - \sigma$ system, the mixing should have the relation:

$$\begin{pmatrix} \sigma \\ f_0 \end{pmatrix} = \begin{pmatrix} \cos\theta & -\sin\theta \\ \sin\theta & \cos\theta \end{pmatrix} \begin{pmatrix} f_n \\ f_s \end{pmatrix}. \tag{13}$$

B. Perturbative calculations

For $\bar{B}_s^0 \to SS$ decay mode, the relevant weak effective Hamiltonian can be written as [29]

$$\mathcal{H}_{\text{eff}} = \frac{G_F}{\sqrt{2}} \left\{ V_{ub} V_{us}^* [C_1(\mu) O_1(\mu) + C_2(\mu) O_2(\mu)] - V_{tb} V_{ts}^* \left[\sum_{i=3}^{10} C_i(\mu) O_i(\mu) \right] \right\}, \tag{14}$$

where $G_F = 1.66378 \times 10^{-5}$ GeV^{-2} is Fermi constant, and $V_{ub}V_{us}^*$ and $V_{tb}V_{ts}^*$ are Cabibbo-Kobayashi-Maskawa (CKM) factors, $O_i(\mu)$ $(i = 1, 2, \ldots, 10)$ is local four-quark operator, which will be listed as follows, and $C_i(\mu)$ is corresponding Wilson coefficient.

(1) Current-current operators (tree):

$$O_1 = (\bar{s}_\alpha u_\beta)_{V-A} (\bar{u}_\beta b_\alpha)_{V-A}, \qquad O_2 = (\bar{s}_\alpha u_\alpha)_{V-A} (\bar{u}_\beta b_\beta)_{V-A}, \tag{15}$$

(2) QCD penguin operators:

$$O_3 = (\bar{s}_\alpha b_\alpha)_{V-A} \sum_q (\bar{q}_\beta q_\beta)_{V-A}, \qquad O_4 = (\bar{s}_\alpha b_\beta)_{V-A} \sum_q (\bar{q}_\beta q_\alpha)_{V-A},$$
$$O_5 = (\bar{s}_\alpha b_\alpha)_{V-A} \sum_q (\bar{q}_\beta q_\beta)_{V+A}, \qquad O_6 = (\bar{s}_\alpha b_\beta)_{V-A} \sum_q (\bar{q}_\beta q_\alpha)_{V+A}, \tag{16}$$

(3) Electroweak penguin operators:

$$O_7 = \frac{3}{2} (\bar{s}_\alpha b_\alpha)_{V-A} \sum_q e_q (\bar{q}_\beta q_\beta)_{V+A}, \qquad O_8 = \frac{3}{2} (\bar{s}_\alpha b_\beta)_{V-A} \sum_q e_q (\bar{q}_\beta q_\alpha)_{V+A},$$
$$O_9 = \frac{3}{2} (\bar{s}_\alpha b_\alpha)_{V-A} \sum_q e_q (\bar{q}_\beta q_\beta)_{V-A}, \qquad O_{10} = \frac{3}{2} (\bar{s}_\alpha b_\beta)_{V-A} \sum_q e_q (\bar{q}_\beta q_\alpha)_{V-A}, \tag{17}$$

with the color indices α, β and $(q\bar{q})_{V\pm A} = \bar{q}\gamma_\mu(1 \pm \gamma_5)q$. The q denotes the u quark and d quark, and e_q is corresponding charge.

The momenta of the $\bar{B}_s^0$, scalar mesons M_1, M_2 in the light-cone coordinate read as

$$p_B = p_1 = \frac{m_{B_s}}{\sqrt{2}}(1, 1, 0_T),$$
$$p_2 = \frac{m_{B_s}}{\sqrt{2}}(r_S^2, 1 - r_S^2, 0_T),$$
$$p_3 = \frac{m_{B_s}}{\sqrt{2}}(1 - r_S^2, r_S^2, 0_T), \tag{18}$$

with the B_s^0 mass m_{B_s} and the mass ratio $r_S = \frac{m_S}{m_{B_s}}$.

And the corresponding light quark's momenta in each meson read as

$$k_1 = (x_1 p_1^+, 0, k_{1T}) = \left(\frac{m_{B_s}}{\sqrt{2}} x_1, 0, k_{1T}\right),$$
$$k_2 = (0, x_2 p_2^-, k_{2T}) = \left(0, \frac{m_{B_s}}{\sqrt{2}}(1 - r_S^2)x_2, k_{2T}\right),$$
$$k_3 = (x_3 p_3^+, 0, k_{3T}) = \left(\frac{m_{B_s}}{\sqrt{2}}(1 - r_S^2)x_3, 0, k_{3T}\right). \tag{19}$$

Then based on the pQCD approach, we can write the decay amplitude as

$$\mathcal{A} \sim \int dx_1 dx_2 dx_3 b_1 db_1 b_2 db_2 b_3 db_3 \times \mathrm{Tr}[H(x_i, b_i, t) C_t \Phi_B(x_1, b_1) \Phi_S(x_2, b_2) \times \Phi_S(x_3, b_3) S_t(x_i) e^{-S(t)}], \tag{20}$$

where b_i is the conjugate momenta of k_i, and t is the largest energy scale in hard function $H(x_i, b_i, t)$. The $e^{-S(t)}$ suppress the soft dynamics [30] and make a reliable perturbative calculation of the hard function H, which come from higher order radiative corrections to wave functions and hard amplitudes. Φ_M represent universal and channel independent wave function, which describes the hadronization of mesons.

As depicted in Fig. 1, we calculate all the contributed diagrams respectively. We use F and M denote the factorizable and nonfactorizable contributions respectively, and the subscript a, c, e, g denote the contributions of the Feynman diagrams (a) and (b), (c) and (d), (e) and (f), (g) and (h) and the superscript LL, LR, SP is the $(V-A)(V-A)$, $(V-A)(V+A)$, and $(S-P)(S+P)$ vertex, respectively. The vertex $(S-P)(S+P)$ is the Fierz transformation of the $(V-A)(V+A)$.

First, the total contribution of the factorization diagrams (a) and (b) with different currents are

(1) $(V-A)(V-A)$

$$F_a^{LL} = 8\pi C_F f_S m_{B_s}^4 \int_0^1 dx_1 dx_2 \times \int_0^\infty b_1 b_2 db_1 db_2 \phi_B(x_1, b_1) \times \{[-(2+x_2)\phi_S(x_2) + r_S(1+2x_2)(\phi_S^S(x_2) + \phi_S^T(x_2))] h_a^1(x_1, x_2, b_1, b_2) E_{ef}(t_a^1) S_t(x_2) + [2r_S \phi_S^S(x_2)] h_a^2(x_1, x_2, b_1, b_2) E_{ef}(t_a^2) S_t(x_1)\}, \tag{21}$$

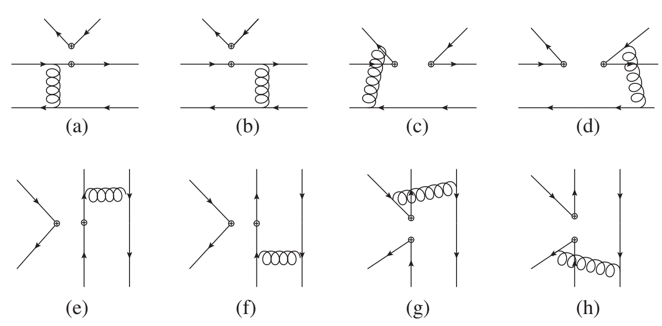

FIG. 1. The lowest order Feynman diagrams of the $\bar{B}_s^0 \to SS$ decays in pQCD approach. The $\bar{B}_s^0 \to a_0 a_0$ decay is the rare decay mode, which only have the last line Feynman diagrams.

(2) $(V-A)(V+A)$

$$F_a^{LR} = F_a^{LL}, \tag{22}$$

(3) $(S-P)(S+P)$

$$\begin{aligned} F_a^{SP} = {} & -16\pi C_F \bar{f}_S m_{B_s}^4 r_S \int_0^1 dx_1 dx_2 \int_0^\infty b_1 b_2 db_1 db_2 \phi_B(x_1, b_1) \\ & \times \{[r_S(5+x_2)\phi_S^S(x_2) + r_S(1-x_2)\phi_S^T(x_2) - 3\phi_S(x_2)] \\ & \times h_a^1(x_1, x_2, b_1, b_2) E_{ef}(t_a^1) S_t(x_2) \\ & - [2r_S(1-x_1)\phi_S^S(x_2) + x_1\phi_S(x_2)] \\ & \times h_a^2(x_1, x_2, b_1, b_2) E_{ef}(t_a^2) S_t(x_1)\}, \end{aligned} \tag{23}$$

with the color factor $C_F = \frac{N_c^2-1}{2N_c} = \frac{4}{3}$. The factorization contribution of the $(V-A)(V-A)$ and $(V-A)(V+A)$ current are neglected because the vector decay constant is a small value and we take it as zero.

For nonfactorization diagrams, the total contribution from (c) and (d) is

(1) $(V-A)(V-A)$

$$\begin{aligned} M_c^{LL} = {} & \frac{32\pi C_F m_{B_s}^4}{\sqrt{2N_c}} \int_0^1 dx_1 dx_2 dx_3 \int_0^\infty b_2 b_3 db_2 db_3 \phi_B(x_1, b_3) \\ & \times \{[(x_3 + x_1 - 1)\phi_S(x_3)\phi_S(x_2) + r_S(1-x_2)\phi_S(x_3)(\phi_S^S(x_2) - \phi_S^T(x_2))] \\ & \times h_c^1(x_1, x_2, x_3, b_2, b_3) E_{nef}(t_c^1) \\ & - [(x_1 + x_2 - x_3 - 1)\phi_S(x_3)\phi_S(x_2) + r_S(1-x_2)\phi_S(x_3)(\phi_S^S(x_2) + \phi_S^T(x_2))] \\ & \times h_c^2(x_1, x_2, x_3, b_2, b_3) E_{nef}(t_c^2)\}, \end{aligned} \tag{24}$$

(2) $(V-A)(V+A)$

$$\begin{aligned} M_c^{LR} = {} & \frac{32\pi C_F m_{B_s}^4}{\sqrt{2N_c}} \int_0^1 dx_1 dx_2 dx_3 \int_0^\infty b_2 b_3 db_2 db_3 \phi_B(x_1, b_3) \\ & \times \{[r_S^2(2 - x_1 - x_2 - x_3)\phi_S^S(x_3)\phi_S^S(x_2) + r_S^2(x_1 - x_2 + x_3)\phi_S^S(x_3)\phi_S^T(x_2) \\ & + r_S^2(x_1 - x_2 + x_3)\phi_S^T(x_3)\phi_S^S(x_2) + r_S^2(2 - x_1 - x_2 - x_3)\phi_S^T(x_3)\phi_S^T(x_2) \\ & + r_S(1 - x_1 - x_3)(\phi_S^S(x_3) - \phi_S^T(x_3))\phi_S(x_2)] \times h_c^1(x_1, x_2, x_3, b_2, b_3) E_{nef}(t_c^1) \\ & - [r_S^2(1 - x_1 - x_2 + x_3)\phi_S^S(x_3)\phi_S^S(x_2) + r_S^2(x_1 - x_2 - x_3 + 1)\phi_S^S(x_3)\phi_S^T(x_2) \\ & - r_S^2(x_1 - x_2 - x_3 + 1)\phi_S^T(x_3)\phi_S^S(x_2) - r_S^2(1 - x_1 - x_2 + x_3)\phi_S^T(x_3)\phi_S^T(x_2) \\ & + r_S(-x_1 + x_3)(\phi_S^S(x_3) + \phi_S^T(x_3))\phi_S(x_2)] \times h_c^2(x_1, x_2, x_3, b_2, b_3) E_{nef}(t_c^2)\}, \end{aligned} \tag{25}$$

(3) $(S-P)(S+P)$

$$\begin{aligned} M_c^{SP} = {} & -\frac{32\pi C_F m_{B_s}^4}{\sqrt{2N_c}} \int_0^1 dx_1 dx_2 dx_3 \int_0^\infty b_2 b_3 db_2 db_3 \phi_B(x_1, b_3) \\ & \times \{[(x_1 + x_2 + x_3 - 2)\phi_S(x_3)\phi_S(x_2) + r_S(1-x_2)\phi_S(x_3)(\phi_S^S(x_2) + \phi_S^T(x_2))] \\ & \times h_c^1(x_1, x_2, x_3, b_2, b_3) E_{nef}(t_c^1) \\ & - [(x_1 - x_3)\phi_S(x_3)\phi_S(x_2) + r_S(1-x_2)\phi_S(x_3)(\phi_S^S(x_2) - \phi_S^T(x_2))] \\ & \times h_c^2(x_1, x_2, x_3, b_2, b_3) E_{nef}(t_c^2)\}, \end{aligned} \tag{26}$$

The total contribution of the annihilation Feynman diagrams Figs. 1(e) and 1(f), which only involve the wave function of the final light scalar mesons, are

(1) $(V-A)(V-A)$

$$\begin{aligned} F_e^{LL} = 8\pi C_F f_B m_{B_s}^4 \int_0^1 dx_2 dx_3 \int_0^\infty b_2 b_3 db_2 db_3 \\ \times \{[-x_3\phi_S(x_3)\phi_S(x_2) + 2r_S^2(1+x_3)\phi_S^S(x_3)\phi_S^S(x_2) - 2r_S^2(1-x_3)\phi_S^T(x_3)\phi_S^S(x_2)] \\ \times h_e^1(x_2,x_3,b_2,b_3)E_{af}(t_e^1)S_t(x_3) \\ + [x_2\phi_S(x_3)\phi_S(x_2) - 2r_S^2(1+x_2)\phi_S^S(x_3)\phi_S^S(x_2) + 2r_S^2(1-x_2)\phi_S^S(x_3)\phi_S^T(x_2)] \\ \times h_e^2(x_2,x_3,b_2,b_3)E_{af}(t_e^2)S_t(x_2)\}, \end{aligned} \tag{27}$$

(2) $(V-A)(V+A)$

$$F_e^{LR} = F_e^{LL}, \tag{28}$$

(3) $(S-P)(S+P)$

$$\begin{aligned} F_e^{SP} = 16\pi C_F f_B m_{B_s}^4 \int_0^1 dx_2 dx_3 \int_0^\infty b_2 b_3 db_2 db_3 \\ \times \{[2r_S\phi_S(x_3)\phi_S^S(x_2) - r_S x_3(\phi_S^S(x_3) - \phi_S^T(x_3))\phi_S(x_2)] \\ \times h_e^1(x_2,x_3,b_2,b_3)E_{af}(t_e^1)S_t(x_3) \\ + [r_S x_2\phi_S(x_3)(\phi_S^S(x_2) - \phi_S^T(x_2)) - 2r_S\phi_S^S(x_3)\phi_S(x_2)] \\ \times h_e^2(x_2,x_3,b_2,b_3)E_{af}(t_e^2)S_t(x_2)\}, \end{aligned} \tag{29}$$

Then the total nonfactorizable annihilation decay amplitudes for the Figs. 1(g) and 1(h) diagrams are

(1) $(V-A)(V-A)$

$$\begin{aligned} M_g^{LL} = \frac{32\pi C_F m_{B_s}^4}{\sqrt{2N_c}} \int_0^1 dx_1 dx_2 dx_3 \int_0^\infty b_1 b_2 db_1 db_2 \phi_B(x_1,b_1) \\ \times \{[-x_2\phi_S(x_2)\phi_S(x_3) - r_S^2(x_1-x_3-x_2)\phi_S^S(x_2)\phi_S^S(x_3) \\ + r_S^2(x_1-x_3+x_2)\phi_S^S(x_2)\phi_S^T(x_3) + r_S^2(x_1-x_3+x_2)\phi_S^T(x_2)\phi_S^S(x_3) \\ - r_S^2(x_1-x_3-x_2)\phi_S^T(x_2)\phi_S^T(x_3)]h_g^1(x_1,x_2,x_3,b_1,b_2)E_{naf}(t_g^1) \\ + [(x_1+x_3)\phi_S(x_2)\phi_S(x_3) - r_S^2(2+x_1+x_3+x_2)\phi_S^S(x_2)\phi_S^S(x_3) \\ + r_S^2(x_2-x_1-x_3)\phi_S^S(x_2)\phi_S^T(x_3) \\ + r_S^2(x_2-x_1-x_3)\phi_S^T(x_2)\phi_S^S(x_3) + r_S^2(2-x_2-x_1-x_3)\phi_S^T(x_2)\phi_S^T(x_3)] \\ \times h_g^2(x_1,x_2,x_3,b_1,b_2)E_{naf}(t_g^2)\}, \end{aligned} \tag{30}$$

(2) $(V-A)(V+A)$

$$\begin{aligned} M_g^{LR} = \frac{32\pi C_F m_{B_s}^4}{\sqrt{2N_c}} \int_0^1 dx_1 dx_2 dx_3 \int_0^\infty b_1 b_2 db_1 db_2 \phi_B(x_1,b_1) \\ \times \{[r_S(x_1-x_3)\phi_S(x_2)(\phi_S^S(x_3) + \phi_S^T(x_3)) - r_S x_2(\phi_S^S(x_2) + \phi_S^T(x_2))\phi_S(x_3)] \\ \times h_g^1(x_1,x_2,x_3,b_1,b_2)E_{naf}(t_g^1) \\ + [r_S(x_1+x_3-2)\phi_S(x_2)(\phi_S^S(x_3) + \phi_S^T(x_3)) - r_S(2-x_2)(\phi_S^S(x_2) + \phi_S^T(x_2))\phi_S(x_3)] \\ \times h_g^2(x_1,x_2,x_3,b_1,b_2)E_{naf}(t_g^2)\}, \end{aligned} \tag{31}$$

(3) $(S-P)(S+P)$

$$
\begin{aligned}
M_g^{SP} = {} & \frac{-32\pi C_F m_{B_s}^4}{\sqrt{2N_c}} \int_0^1 dx_1 dx_2 dx_3 \int_0^\infty b_1 b_2 db_1 db_2 \phi_B(x_1,b_1) \\
& \times \{[(-x_1+x_3)\phi_S(x_2)\phi_S(x_3) + r_S^2(x_1-x_3-x_2)\phi_S^S(x_2)\phi_S^S(x_3) \\
& + r_S^2(x_1+x_2-x_3)\phi_S^S(x_2)\phi_S^T(x_3) + r_S^2(x_1+x_2-x_3)\phi_S^T(x_2)\phi_S^S(x_3) \\
& + r_S^2(x_1-x_3-x_2)\phi_S^T(x_2)\phi_S^T(x_3)] h_g^1(x_1,x_2,x_3,b_1,b_2) E_{naf}(t_g^1) \\
& + [-x_2\phi_S(x_2)\phi_S(x_3) + r_S^2(2+x_1+x_3+x_2)\phi_S^S(x_2)\phi_S^S(x_3) \\
& - r_S^2(x_1+x_3-x_2)\phi_S^S(x_2)\phi_S^T(x_3) - r_S^2(x_1+x_3-x_2)\phi_S^T(x_2)\phi_S^S(x_3) \\
& + r_S^2(-2+x_1+x_2+x_3)\phi_S^T(x_2)\phi_S^T(x_3)] \\
& \times h_g^2(x_1,x_2,x_3,b_1,b_2) E_{naf}(t_g^2)\}.
\end{aligned} \tag{32}
$$

For the $\bar{B}_s^0 \to a_0^+ a_0^-$ decay, which is a rare decay mode and only have annihilation Feynman diagrams, the decay amplitude of $\bar{B}_s^0 \to a_0^+ a_0^-$ decay is then

$$
\mathcal{A}(\bar{B}_s^0 \to a_0^+ a_0^-) = V_{ub} V_{us}^* [C_2 M_g^{LL}] - V_{tb} V_{ts}^* \left[\left(2C_4 + \frac{1}{2} C_{10}\right) M_g^{LL} + \left(2C_6 + \frac{1}{2} C_8\right) M_g^{SP}\right]. \tag{33}
$$

Meanwhile, the relationship with respect to the decay $\bar{B}_s^0 \to a_0^0 a_0^0$ is

$$
\sqrt{2}\mathcal{A}(\bar{B}_s^0 \to a_0^0 a_0^0) = \mathcal{A}(\bar{B}_s^0 \to a_0^+ a_0^-) \tag{34}
$$

For the $\bar{B}_s^0 \to f_0 f_0(\sigma\sigma)$ decay, based on the mixing scheme the decay amplitude can be written as:

$$
\begin{aligned}
\sqrt{2}\mathcal{A}(\bar{B}_s^0 \to f_0 f_0) &= \sin^2\theta \mathcal{A}(\bar{B}_s^0 \to f_n f_n) + \sin 2\theta \mathcal{A}(\bar{B}_s^0 \to f_n f_s) + \cos^2\theta \mathcal{A}(\bar{B}_s^0 \to f_s f_s), \\
\sqrt{2}\mathcal{A}(\bar{B}_s^0 \to \sigma\sigma) &= \cos^2\theta \mathcal{A}(\bar{B}_s^0 \to f_n f_n) - \sin 2\theta \mathcal{A}(\bar{B}_s^0 \to f_n f_s) + \sin^2\theta \mathcal{A}(\bar{B}_s^0 \to f_s f_s).
\end{aligned} \tag{35}
$$

with

$$
\begin{aligned}
\mathcal{A}(\bar{B}_s^0 \to f_s f_s) = {} & -2V_{tb} V_{ts}^* \left[\left(a_3 + a_4 + a_5 - \frac{1}{2} a_7 - \frac{1}{2} a_9 - \frac{1}{2} a_{10}\right) f_B M_e^{LL} + \left(a_6 - \frac{1}{2} a_8\right) (F_a^{SP} \bar{f}_S + F_e^{SP} f_B)\right. \\
& + \left(C_3 + C_4 - \frac{1}{2} C_9 - \frac{1}{2} C_{10}\right)(M_c^{LL} + M_g^{LL}) + \left(C_5 - \frac{1}{2} C_7\right)(M_c^{LR} + M_g^{LR}) \\
& \left. + \left(C_6 - \frac{1}{2} C_8\right)(M_c^{SP} + M_g^{SP})\right]
\end{aligned} \tag{36}
$$

$$
\sqrt{2}\mathcal{A}(\bar{B}_s^0 \to f_n f_s) = -V_{tb} V_{ts}^* \left[\left(C_4 - \frac{1}{2} C_{10}\right) M_c^{LL} + \left(C_6 - \frac{1}{2} C_8\right) M_c^{SP}\right] \tag{37}
$$

and the decay amplitude of the $\bar{B}_s^0 \to f_n f_n$ is same to the $\bar{B}_s^0 \to a_0 a_0$ decays. For the considered decay modes, the corresponding decay width is

$$
\Gamma(\bar{B}_s^0 \to SS) = \frac{G_F^2 m_{B_s}^3}{128\pi} (1 - 2r_S^2) |\mathcal{A}(\bar{B}_s^0 \to SS)|^2. \tag{38}
$$

Here, it is noticeable that the contribution from the factorizable annihilation diagrams in the $B_s^0 \to a_0 a_0$ decay is very small and can be safely neglected due to the isospin symmetry. And owing to the decay constant of the scalar meson $f_S = 0$, we neglect all the responding contribution in our calculation.

III. NUMERICAL RESULTS AND DISCUSSIONS

In this section, we will calculate the CP-averaged branching ratios and CP-violation asymmetries for the $\bar{B}_s^0 \to SS$ decays and make some analyses about the results. First, we list the input parameters that are used in the calculations below. The masses and decay constant of the mesons, the lifetime of the B_s are [19,31,32]

$$\begin{aligned} &m_{B_s} = 5.367 \text{ GeV}, \quad \bar{m}_b(\bar{m}_b) = 4.2 \text{ GeV}, \quad m_{a_0} = 0.98 \pm 0.02 \text{ GeV}, \\ &m_{f_0} = 0.99 \pm 0.02 \text{ GeV}, \quad f_{B_s} = 227.2 \pm 3.4 \text{ MeV}, \quad \tau_{B_s} = 1.509 \text{ ps}, \\ &m_{f_n} = 0.99 \text{ GeV}, \quad m_{f_s} = 1.02 \text{ GeV} \quad m_\sigma = 0.5 \text{ GeV}. \end{aligned} \tag{39}$$

and in the CKM matrix elements, the involved Wolfenstein parameters are

$$\begin{aligned} &\lambda = 0.22453 \pm 0.00044, \quad A = 0.836 \pm 0.015, \\ &\bar{\rho} = 0.122^{+0.018}_{-0.017}, \quad \bar{\eta} = 0.355^{+0.012}_{-0.011}. \end{aligned} \tag{40}$$

with the relations $\bar{\rho} = \rho(1 - \frac{\lambda^2}{2})$ and $\bar{\eta} = \eta(1 - \frac{\lambda^2}{2})$.

A. Branching Ratios

In this section, we separately give the results of the three considered decays $B_s^0 \to a_0 a_0$, $B_s^0 \to f_0 f_0$, and $B_s^0 \to \sigma\sigma$. For the $B_s^0 \to a_0 a_0$, this decay mode have both tree operators and penguin operators in the quark level. In SM, the γ angle is associated with the CKM matrix element V_{ub}, which have the relationship $V_{ub} \simeq |V_{ub}| e^{-i\gamma}$. So we can leave the CKM phase angle γ as an unknown parameter, and write the decay amplitude of the $\bar{B}_s^0 \to a_0 a_0$ decay as

$$\bar{\mathcal{A}} = V_{ub} V_{us}^* T - V_{tb} V_{ts}^* P = V_{ub} V_{us}^* T (1 + z e^{i(\delta+\gamma)}), \tag{41}$$

where the ratio $z = |V_{tb} V_{ts}^* / V_{ub} V_{us}^*| \cdot |P/T|$, and δ is the relative strong phase between the tree amplitudes(T) and penguin amplitudes (P). The value of z and δ can be calculated from the pQCD.

Meanwhile, the decay amplitude of the conjugated decay mode $B_s^0 \to a_0 a_0$ can be written by replacing $V_{ub} V_{us}^*$ with $V_{ub}^* V_{us}$ and $V_{tb} V_{ts}^*$ with $V_{tb}^* V_{ts}$ as

$$\mathcal{A} = V_{ub}^* V_{us} T - V_{tb}^* V_{ts} P = V_{ub}^* V_{us} T (1 + z e^{i(\delta-\gamma)}). \tag{42}$$

Then from Eqs. (41) and (42), the CP-averaged decay width of $\bar{B}_s^0(B_s^0) \to a_0^+ a_0^-$ is

$$\begin{aligned} \Gamma(\bar{B}_s^0(B_s^0) \to a_0^+ a_0^-) &= \frac{G_F^2 m_{B_s}^3}{256\pi} (1 - 2r_{a_0}^2)(|\mathcal{A}|^2 + |\bar{\mathcal{A}}|^2) \\ &= \frac{G_F^2 m_{B_s}^3}{128\pi} (1 - 2r_{a_0}^2) |V_{ub}^* V_{us} T|^2 \\ &\quad \times (1 + 2z\cos(\gamma)\cos(\delta) + z^2). \end{aligned} \tag{43}$$

In Fig. 2, we plot the average branching ratio of the decay $\bar{B}_s^0 \to a_0^+ a_0^-$ and $\bar{B}_s^0 \to a_0^0 a_0^0$ about the parameter γ

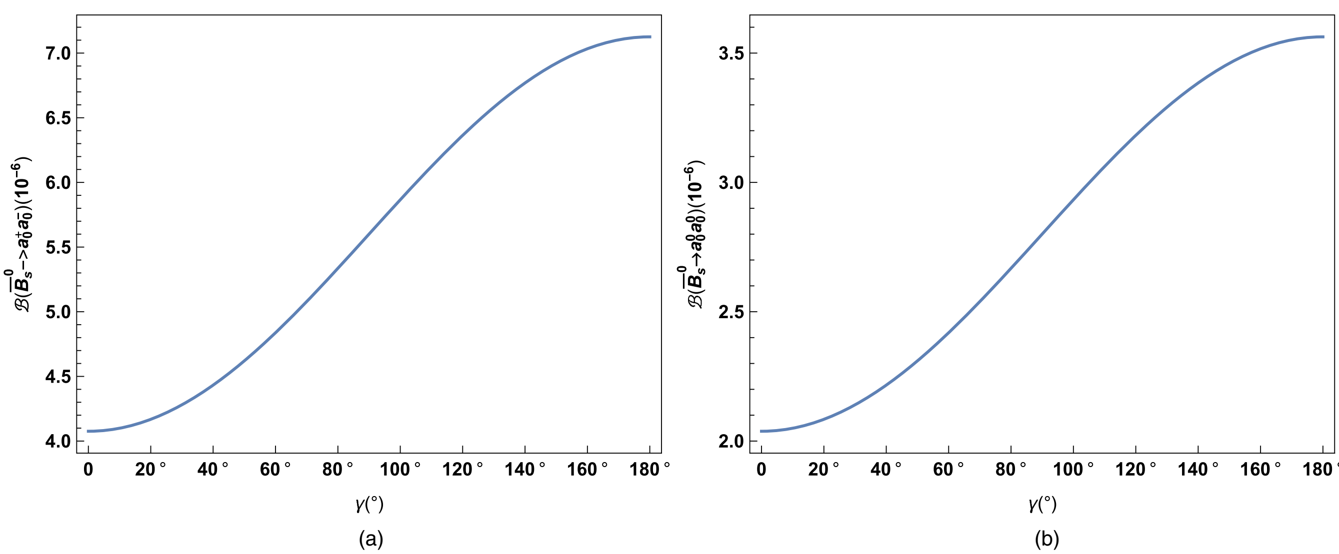

FIG. 2. (a) The branching ratio of the $\bar{B}_s^0 \to a_0^+ a_0^-$ decay as a function of γ; (b) The branching ratio of the $\bar{B}_s^0 \to a_0^0 a_0^0$ decay as a function of γ.

respectively. Since the CKM angle γ is constrained as γ around 73.5° in Review of Particle Physics [19],

$$\gamma = (73.5^{+4.2}_{-5.1})^\circ \tag{44}$$

we get from Fig. 2 when we take γ as $70^\circ \sim 80^\circ$,

$$5.08\times 10^{-6} < \mathcal{B}(\bar{B}_s^0 \to a_0^+ a_0^-) < 5.34\times 10^{-6}; \tag{45}$$

$$2.54\times 10^{-6} < \mathcal{B}(\bar{B}_s^0 \to a_0^0 a_0^0) < 2.67\times 10^{-6}. \tag{46}$$

The value of $z = 6.67$ indicate that the amplitude of the penguin diagrams is almost 6.67 times of that of tree diagrams. Therefore the main contribution come from the penguin diagrams in this decays, which enhance the results of the branching ratios.

When we utilize the input parameters and decay amplitudes, furthermore leave the phase angle γ aside, it is easy to get the CP-average branching ratios for both containing the charged and neutral scalar mesons decay modes, which are

$$\mathcal{B}(\bar{B}_s^0 \to a_0^+ a_0^-) = 5.17^{+1.62}_{-1.39}(B_1)^{+0.24}_{-0.09}(B_3)^{+1.23}_{-1.03}(\bar{f}_{a_0})^{+0.63}_{-0.55}(\omega_b)^{+0.99}_{-0.67}(t_i)\times 10^{-6}, \tag{47}$$

$$\mathcal{B}(\bar{B}_s^0 \to a_0^0 a_0^0) = 2.58^{+0.81}_{-0.63}(B_1)^{+0.12}_{-0.04}(B_3)^{+0.62}_{-0.52}(\bar{f}_{a_0})^{+0.31}_{-0.27}(\omega_b)^{+0.50}_{-0.33}(t_i)\times 10^{-6}. \tag{48}$$

In pQCD approach, the wave functions of the initial and final mesons, whose are universal and channel independent, are the dominant inputs and have an important influence on the numerical results. As it has been shown above, the primary errors come from the uncertainties of Gegenbauer moments $B_1 = -0.93 \pm 0.10$ and $B_3 = 0.14 \pm 0.08$, the scalar decay constant $\bar{f}_{a_0} = 0.365 \pm 0.020$ GeV, the shape parameter $\omega_b = 0.50 \pm 0.05$, and the hard scale t_i, respectively. The hard scale t_i varies from $0.8t \sim 1.2t$ (not changing $1/b_i$, $i = 1, 2, 3$), which characterizes the size of the next-leading-order contribution. The errors from the other uncertainties, such as the mass of the m_{a_0} and CKM matrix elements, turn out to be small and can be neglected. It is apparent that the main errors are caused by the nonperturbative input parameters, which we need more precise experimental data to determine. By adding all of these vital uncertainties in quadrature, we get $\mathcal{B}(\bar{B}_s^0 \to a_0^+ a_0^-) = (5.17^{+2.36}_{-1.94})\times 10^{-6}$ and $\mathcal{B}(\bar{B}_s^0 \to a_0^0 a_0^0) = (2.58^{+1.18}_{-0.92})\times 10^{-6}$.

In our previous work of $B_s^0 \to \pi^+\pi^-$ [33](one of the author have recalculated the $B_s^0 \to \pi^+\pi^-$ and $B^0 \to K^+K^-$ in 2012 [34]), the theoretical results of these two decay modes are $\mathcal{B}(B_s^0 \to \pi^+\pi^-) = 5.10\times 10^{-7}$ and $\mathcal{B}(B^0 \to K^+K^-) = 1.56\times 10^{-7}$, where the corresponding experimental results about the branching ratios [35,36] of these two decay modes approximately at the order of the $10^{-7} \sim 10^{-8}$. The predicted results of $\bar{B}_s^0 \to a_0 a_0$ for both charged and neutral a_0 mesons, however, are at the order of 10^{-6} although these decay modes have the same quark components for both initial and final state mesons and the only pure annihilation contributions. So this results push us to make some comments about why the branching ratio of the $\bar{B}_s^0 \to a_0^+ a_0^-$ is more large than the results of the $B_s^0 \to \pi^+\pi^-$ decay and $B^0 \to K^+K^-$ decay. By comparison, we can first find that the main underlying reason is that the QCD dynamics of the scalar meson a_0 is different from that of the pseudoscalar meson π and K, where at the leading twist the scalar meson a_0 is dominated by the odd Gegenbauer polynomials but the pseudoscalar mesons both π and K are governed by the even Gegenbauer polynomials. Second the decay constant $\bar{f}_{a_0}$ is about two times than the decay constants of the f_π and f_K [34,37]. These two reasons lead to the nonfactorizable annihilation contribution is more large in the $\bar{B}_s^0 \to a_0 a_0$ mode. In Table I, we list the decay amplitudes of the $\bar{B}_s^0 \to a_0 a_0$ for different distribution amplitudes of twist-2 or twist-3, and also we list the results of Ref. [34] about the decay mode $B^0 \to K^+K^-$ for contrast. From Table I, it is obvious that the twist-2 DA make dominant contribution, and the decay amplitudes of the $\bar{B}_s^0 \to a_0 a_0$ decay is approximately one order of the magnitude larger than that of the $B^0 \to K^+K^-$.

For the $\bar{B}_s^0 \to f_0 f_0$ decay, it is governed by the $b \to s s \bar{s}$ when we regard f_0 as the $s\bar{s}$, and this type decay only have the penguin operators due to the fact that the tree operators are forbidden. When introducing the mixing effect from the component of the $(u\bar{u} + d\bar{d})/\sqrt{2}$, we take the mixing angle θ as a free parameter, and then plot the branching ratio's dependence on the mixing angle in Fig. 3. If the f_0 is the pure $s\bar{s}$ component, namely the mixing angle $\theta = 0^\circ$, the branching ratio of the $\bar{B}_s^0 \to f_0 f_0$

TABLE I. The different source of twist-2 and twist-3 contribution.

Decay mode	Twist-2 $\phi_{a_0}(\phi_K^A)$	Twist-3 $\phi_{a_0}^S(\phi_K^P)$	Twist-3 $\phi_{a_0}^T(\phi_K^T)$
$\mathcal{A}(\bar{B}_s^0 \to a_0^+ a_0^-)$	$(-2.0 - 2.1i)\times 10^{-4}$	$(+4.2 + 4.1i)\times 10^{-5}$	$(-2.27 - 0.79i)\times 10^{-6}$
$\mathcal{A}(B^0 \to K^+K^-)$ [34]	$(-0.31 - 2.2i)\times 10^{-5}$	$(-0.61 - 0.55i)\times 10^{-5}$	$(-0.06 - 0.27i)\times 10^{-5}$

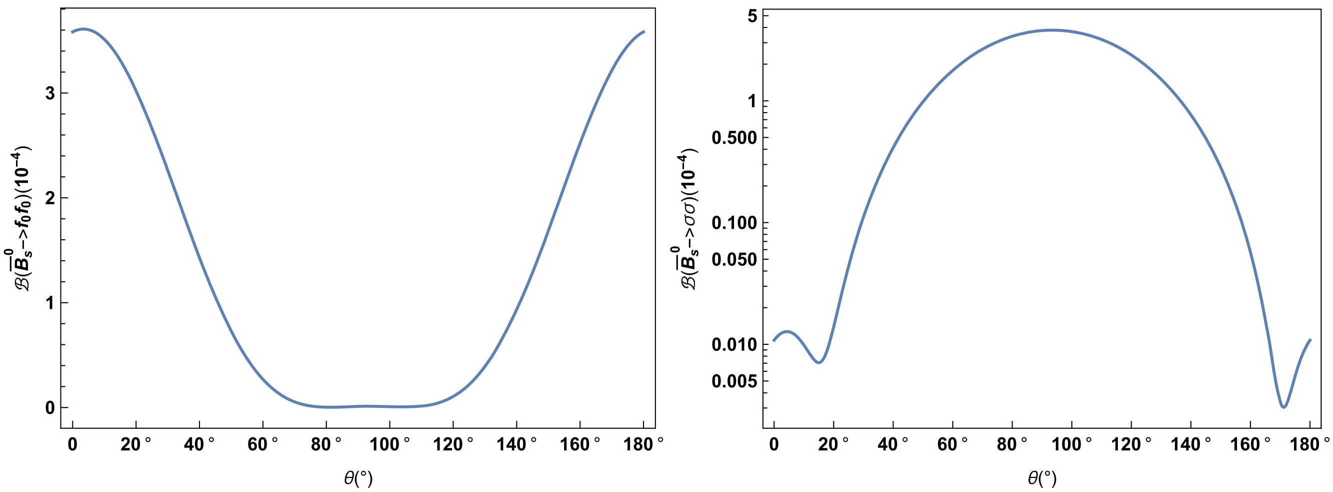

(a) (b)

FIG. 3. (a) The branching ratio of the $\bar{B}_s^0 \to f_0 f_0$ decay as a function of mixing angle θ; (b) The branching ratio of the $\bar{B}_s^0 \to \sigma\sigma$ decay as a function of mixing angle θ.

is approximately 3.6×10^{-4}, and when including the mixing effect of the $(u\bar{u}+d\bar{d})/\sqrt{2}$, the result changes clearly which we can read from Fig. 3(a). For the $\bar{B}_s^0 \to \sigma\sigma$ decay, there are still a lot of uncertainties about the wave function of σ meson, we choose the same decay constant for f_n and f_s in our calculations, just as it has been done in Ref. [8]. The results of this decay is contrary to the $\bar{B}_s^0 \to f_0 f_0$, which is dominated by the sin law that we just see from the Eq. (35), when taking the mixing angle $\theta = 0°$, the branching ratio of this decay is very small, and it will increase about one or two magnitudes in consideration of the mixing effect of the $s\bar{s}$. The decay amplitude of the $\bar{B}_s^0 \to f_0 f_0(\sigma\sigma)$ contain three parts, $f_n f_n$, $f_n f_s$, and $f_s f_s$, and the main contribution comes from $f_s f_s$. The oscillation near the two ends of the θ-coordinate in Fig. 3(b) mainly due to the interference from $\bar{B}_s^0 \to f_n f_n$ and its contribution obey the cos law for $\bar{B}_s^0 \to \sigma\sigma$ decay that will obviously enhance the two ends of theta axis in Fig. 3(b). Taking both decays into account, we can find that the mixing angle can be constrained in the range [19°, 66°] and [119°, 166°] because it will be nearly zero when taking other values, and if combining the known results that obtained from the experiment, the range will be smaller. The mixing angle range that we get is also consistent with the data of the Refs. [38–41].

The mixing angle is not clear up to now, and there are a lot of works to constrain the angle range. The LHCb Collaboration first announced the upper limit $|\theta| < 31°$ for the mixing angle of the $\sigma - f_0$ in Ref. [42]. So we set the two value $\theta = 25°$ and $\theta = 30°$ to make some calculation respectively, the branching ratios are presented as

(1) $\theta = 25°$

$$\begin{aligned}\mathcal{B}(\bar{B}_s^0 \to f_0 f_0) &= 2.66^{+0.19}_{-0.18}(B_1)^{+0.31}_{-0.29}(B_3)^{+0.63}_{-0.53}(\bar{f}_S)^{+0.32}_{-0.27}(\omega_b)^{+0.73}_{-0.50}(t_i)\times10^{-4},\\ &= 2.66^{+1.08}_{-0.85}\times10^{-4};\\ \mathcal{B}(\bar{B}_s^0 \to \sigma\sigma) &= 4.35^{+0.22}_{-0.14}(B_1)^{+0.41}_{-0.37}(B_3)^{+0.52}_{-0.87}(\bar{f}_S)^{+1.00}_{-0.83}(\omega_b)^{+1.25}_{-0.80}(t_i)\times10^{-6}\\ &= 4.35^{+1.75}_{-1.50}\times10^{-6}.\end{aligned} \tag{49}$$

(2) $\theta = 30°$

$$\begin{aligned}\mathcal{B}(\bar{B}_s^0 \to f_0 f_0) &= 2.26^{+0.16}_{-0.16}(B_1)^{+0.26}_{-0.26}(B_3)^{+0.53}_{-0.45}(\bar{f}_S)^{+0.26}_{-0.23}(\omega_b)^{+0.61}_{-0.42}(t_i)\times10^{-4}\\ &= 2.26^{+0.90}_{-0.72}\times10^{-4},\\ \mathcal{B}(\bar{B}_s^0 \to \sigma\sigma) &= 1.11^{+0.04}_{-0.04}(B_1)^{+0.01}_{-0.02}(B_3)^{+0.21}_{-0.22}(\bar{f}_S)^{+0.21}_{-0.18}(\omega_b)^{+0.32}_{-0.21}(t_i)\times10^{-5}\\ &= 1.11^{+0.44}_{-0.36}\times10^{-5}.\end{aligned} \tag{50}$$

We can get the same results when the value of θ are close to the 161° and 157°, respectively. In every second line of the Eqs. (49) and (50), the theoretical errors that we considered are added in quadrature. The main reason for the branching ratio of $\bar{B}_s^0 \to f_0 f_0$ is larger than that of $\bar{B}_s^0 \to \sigma\sigma$ is that the mass of f_0 is almost one time heavier than that of σ.

For the mixing of $a_0^0 - f_0$, we directly take the mixing intensity ξ_{fa},

$$\xi_{fa} = (0.99 \pm 0.16 \pm 0.30 \pm 0.19) \times 10^{-2} \quad (\text{solution I}),$$
$$\xi_{fa} = (0.41 \pm 0.13 \pm 0.17 \pm 0.13) \times 10^{-2} \quad (\text{solution II}). \tag{51}$$

which are first measured in the BESIII collaboration [21], and the relation $|\xi_{fa}| \simeq \tan^2\phi$ is applied to get the mixing angle ϕ [43].

$$\phi = (5.45 \pm 1.65)° \quad (\text{solution I}),$$
$$\phi = (3.02 \pm 2.21)° \quad (\text{solution II}). \tag{52}$$

From the value, we can conclude that the mixing angle is so small that it will not change our results largely.

Here we also make some comments when the final state of the decay mode treated as the four-quark structure. As we mentioned in the introduction, there is an open problem that the inner structure of the scalar meson are not well identified. In this work, we regard a_0, f_0 and σ as the $q\bar{q}$ in the traditional quark model and make some calculations within the perturbative QCD approach. But when we want to make some predictions of the tetraquark picture in the perturbative QCD approach, we cannot make direct computations because we do not known the necessary physical quantities, such as the wave function of the scalar mesons of the four-quark picture. However, we can image a picture is that the other $q\bar{q}$ pairs must be extracted from the sea quarks when the scalar mesons are four-quark state, and it would be expected that the branching ratios of these decay modes in tetraquark picture are smaller than that in two-quark model.

B. *CP* violation parameters

Now, we will calculate the *CP* violation parameters of the $\bar{B}_s^0 \to a_0 a_0$ decays in this subsection. The *CP* violation parameters of the $\bar{B}_s^0 \to a_0 a_0$ for both charged and neutral a_0 mesons are same because the decay amplitude of these two decay modes are similar and the factor in the front of the decay width formula can be reduced. In SM, *CP* violation originated from the CKM weak angle. For the neutral B_s^0 meson decays, we should take the effect of $\bar{B}_s^0 - B_s^0$ mixing into account, and the time dependent *CP* violation parameters of the two $\bar{B}_s^0 \to a_0 a_0$ decays with charged and neutral scalar mesons can be defined as

$$\begin{aligned} A_{\rm CP} &= \frac{\Gamma(B_s^0(\Delta t) \to a_0 a_0) - \Gamma(\bar{B}_s^0(\Delta t) \to a_0 a_0)}{\Gamma(B_s^0(\Delta t) \to a_0 a_0) + \Gamma(\bar{B}_s^0(\Delta t) \to a_0 a_0)} \\ &= A_{\rm CP}^{\rm dir} \cos(\Delta m \Delta t) + A_{\rm CP}^{\rm mix} \sin(\Delta m \Delta t), \end{aligned}$$

where Δm is the mass difference between the two neutral $B_s^0(\bar{B}_s^0)$ mass eigenstates, and $\Delta t = t_{CP} - t_{tag}$ is the time difference between the tagged $B_s^0(\bar{B}_s^0)$ and the accompanying $\bar{B}_s^0(B_s^0)$ with opposite b flavor decaying to the final *CP* eigenstate $a_0 a_0$ at the time t_{CP}.

From Eqs. (41) and (42), the direct *CP* violation parameter $A_{\rm CP}^{\rm dir}$ can be parametrized as

$$A_{\rm CP}^{\rm dir} = \frac{|A|^2 - |\bar{A}|^2}{|A|^2 + |\bar{A}|^2} = \frac{2z \sin(\delta)\sin(\gamma)}{1 + 2z\cos(\delta)\cos(\gamma) + z^2}. \tag{53}$$

It is obvious that the $A_{\rm CP}^{\rm dir}$ is approximately proportional to CKM angle $\sin(\gamma)$, strong phase $\sin(\delta)$, and the relative size z between the penguin contribution and tree contribution. We plot the direct *CP* violation parameter $A_{\rm CP}^{\rm dir}$ as the function of the weak angle γ in Fig. 4, and one can see that the $A_{\rm CP}^{\rm dir}$ is approximately -11.4% at the peak when the γ is $70° < \gamma < 80°$. The relative small direct *CP* asymmetry is also a result of the main contributions coming from penguin diagrams in this decays.

The involved mixing-induced *CP* violation parameter $A_{\rm CP}^{\rm mix}$ can be written as

$$A_{CP}^{\rm mix} = \frac{-2{\rm Im}(\lambda_{CP})}{1 + |\lambda_{CP}|^2}, \tag{54}$$

with the *CP* violation parameters λ_{CP}

$$\lambda_{CP} = \eta_{CP} \frac{V_{tb}^* V_{ts}}{V_{tb} V_{ts}^*} \frac{\langle a_0 a_0 | H_{\rm eff} | \bar{B}_s^0 \rangle}{\langle a_0 a_0 | H_{\rm eff} | B_s^0 \rangle} = e^{-2i\gamma} \frac{1 + z e^{i(\delta+\gamma)}}{1 + z e^{i(\delta-\gamma)}}, \tag{55}$$

in which η_{CP} is the *CP*-eigenvalue of the final state.

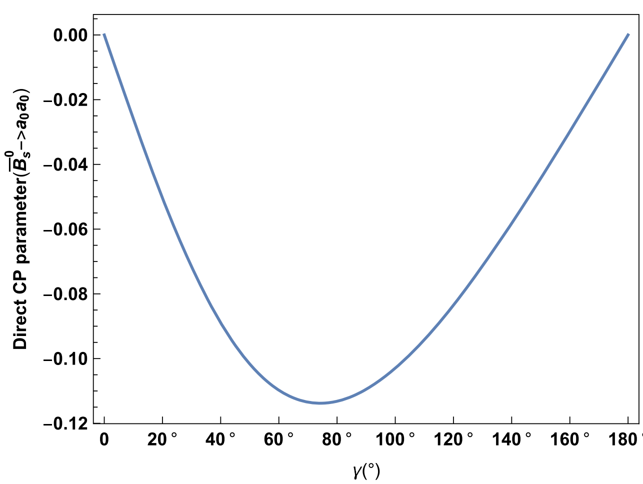

FIG. 4. The direct *CP* violation parameter of the $\bar{B}_s^0(B_s^0) \to a_0 a_0$ decay as a function of γ.

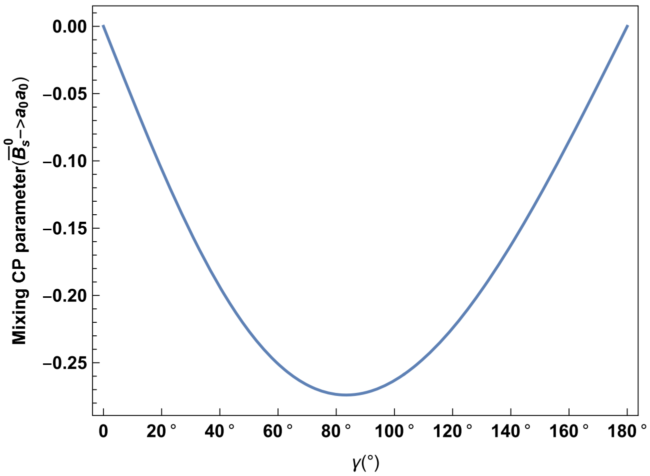

FIG. 5. The mixing CP violation parameter of the $\bar{B}_s^0(B_s^0) \to a_0a_0$ decay as a function of γ.

If z is a very small number, i.e., the penguin diagram contribution is suppressed comparing with the tree diagram contribution, the mixing induced CP asymmetry parameter A_{CP}^{mix} is proportional to $\sin 2\gamma$, which will be a good place for the CKM angle γ measurement. However as we have already mentioned, $z(=6.67)$ is large. We give the mixing CP asymmetry in Fig. 5, one can see that A_{CP}^{mix} just like the case of direct CP violation, it is almost symmetric and the symmetry axis is near $\gamma = \pi/2$. It is close to -27.0% when the angle γ is constrained as γ around $73.5°$. At present, there are no CP asymmetry measurements in experiment but the possible large CP violation we predict for $\bar{B}_s^0 \to a_0a_0$ decays might be observed in the coming LHC-b experiments.

For the $\bar{B}_s^0 \to f_0f_0$ decay, it is a pure penguin process when we regard f_0 as $s\bar{s}$ state and in this case, there is no weak phase that leads the direct CP violation parameter

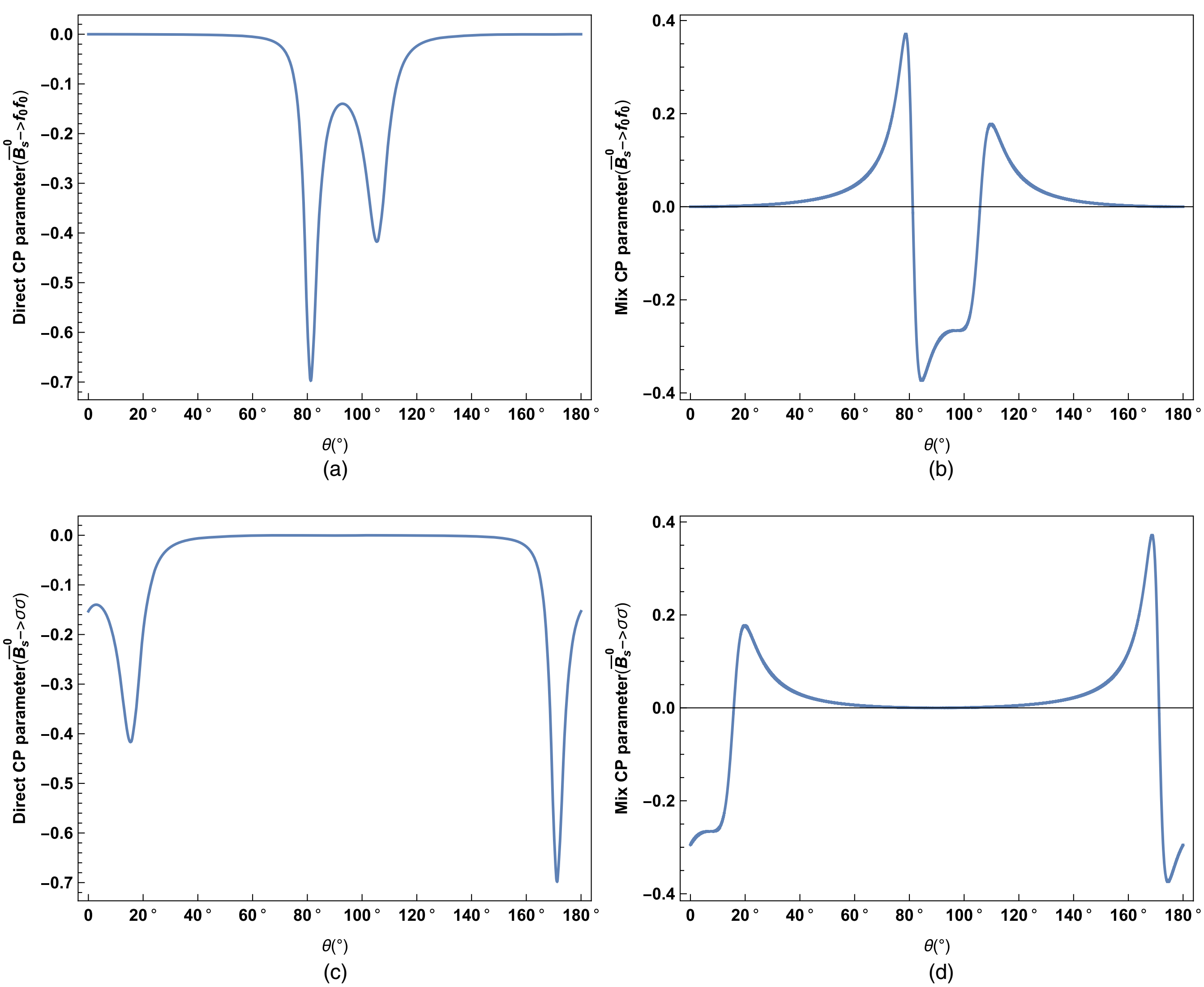

FIG. 6. The direct and mixing CP violation parameter of the $\bar{B}_s^0(B_s^0) \to f_0f_0$ and $\bar{B}_s^0(B_s^0) \to \sigma\sigma$ as a function of mixing angle θ.

equal to zero. Furthermore, it is very small when we take the mixing of the $(u\bar{u}+d\bar{d})/\sqrt{2}$ into account. For the $\bar{B}_s^0\to\sigma\sigma$ decay, it is a rare mode, the CKM matrix elements $|V_{us}V_{ub}|\ll|V_{ts}V_{tb}|$, which make the tree amplitudes are suppressed. From Eq. (53), the direct and mixing CP asymmetries can be defined as follows:

$$A_{\rm CP}^{\rm dir}=\frac{1-|\lambda_{CP}|^2}{1+|\lambda_{CP}|^2},\qquad A_{\rm CP}^{\rm mix}=\frac{-2{\rm Im}(\lambda_{CP})}{1+|\lambda_{CP}|^2},\tag{56}$$

Based on the mixing scheme, we give the CP asymmetries' dependence on the mixing angle θ in Fig. 6.

Here, we use the same value of the $\theta=25°$ to make some prediction,

$$\begin{aligned}A_{\rm CP}^{\rm dir}(\bar{B}_s^0\to f_0f_0)&=0,\\ A_{\rm CP}^{\rm mix}(\bar{B}_s^0\to f_0f_0)&=0.3\%,\\ A_{\rm CP}^{\rm dir}(\bar{B}_s^0\to\sigma\sigma)&=-6.0\%,\\ A_{\rm CP}^{\rm mix}(\bar{B}_s^0\to\sigma\sigma)&=11.7\%,\end{aligned}\tag{57}$$

As for the $\bar{B}_s^0\to f_0f_0$, if we consider f_0 as a pure $s\bar{s}$ state, there is no CP violations; if we consider it as a mixing between $s\bar{s}$ and $q\bar{q}$, we find the interference has little influence on the CP violation parameters. Because the mixing angle cannot be determined in a direct method, our results also can be used to constrain the range of the mixing angle θ if it were observed in the experiment.

IV. SUMMARY

In this paper, we make predictions of the decay $\bar{B}_s^0\to SS(S=a_0(980),f_0(980,500))$ within the pQCD approach for the first time. Basing on the recently experimental results which provide a direct information about the constituent two-quark components in the corresponding a_0 wave function and the theoretical presentations of the scalar meson in scenario 1 , we calculate the branching ratios and CP violation parameters of the decay $\bar{B}_s^0\to a_0a_0$ for both charged and neutral a_0 states and the decay $\bar{B}_s^0\to f_0(\sigma)f_0(\sigma)$. Our calculations show that: (1) the $\bar{B}_s^0\to a_0a_0$ decay modes have relative large branching ratios, which are $\mathcal{B}(\bar{B}_s^0\to a_0^+a_0^-)=(5.17^{+2.36}_{-1.94})\times10^{-6}$ and $\mathcal{B}(\bar{B}_s^0\to a_0^0a_0^0)=(2.58^{+1.18}_{-0.92})\times10^{-6}$, and there is also large CP violation in the decay model; (2) the branching fraction of $\bar{B}_s^0\to f_0(\sigma)f_0(\sigma)$ are at the order of the 10^{-4} (10^{-6}). Because the mixing angle cannot be determined in a direct method, our results also can be used to constrain the range of the mixing angle θ if it were observed in the experiment. In the end, we hope the results can be tested by the running LHC-b experiments in the near future, and, of course, it would help us to get a better understanding of the QCD behavior of the scalar mesons.

ACKNOWLEDGMENTS

The authors would like to thank Dr. Ming-Zhen Zhou and Dr. Shan Cheng for some valuable discussions. This work is supported by the National Natural Science Foundation of China under Grant No. 11047028 and No. 11875226, and by the Fundamental Research Funds of the Central Universities, Grant No. XDJK2012C040.

APPENDIX: FORMULAS FOR THE CALCULATION USED IN THE TEXT

In this part, we list some formulas that are used in the above calculations. The hard scattering kernels function $h_i(i=a,c,e,g)$ involved in the above expression are written as:

$$h_a^1(x_1,x_2,b_1,b_2)=K_0(M_{B_s}b_1\sqrt{x_1(1-x_2)})\times[\theta(b_2-b_1)I_0(M_{B_s}b_1\sqrt{1-x_2})K_0(M_{B_s}b_2\sqrt{1-x_2})+(b_2\leftrightarrow b_1)],\tag{A1}$$

$$h_a^2(x_1,x_2,b_1,b_2)=K_0(M_{B_s}b_2\sqrt{x_1(1-x_2)})\times[\theta(b_2-b_1)I_0(M_{B_s}b_1\sqrt{x_1})K_0(M_{B_s}b_2\sqrt{x_1})+(b_2\leftrightarrow b_1)],\tag{A2}$$

$$\begin{aligned}h_c^1(x_1,x_2,x_3,b_2,b_3)&=[\theta(b_2-b_3)I_0(M_{B_s}b_3\sqrt{x_1(1-x_2)})K_0(M_{B_s}b_2\sqrt{x_1(1-x_2)})+(b_2\leftrightarrow b_3)]\\&\times\begin{cases}K_0(M_{B_s}b_3\sqrt{x_1+x_2+x_3-x_1x_2-x_2x_3-1}), & x_1+x_2+x_3-x_1x_2-x_2x_3-1\geq0\\ \frac{i\pi}{2}H_0^{(1)}(M_{B_s}b_3\sqrt{|x_1+x_2+x_3-x_1x_2-x_2x_3-1|}), & x_1+x_2+x_3-x_1x_2-x_2x_3-1<0\end{cases}\end{aligned}\tag{A3}$$

$$\begin{aligned}h_c^2(x_1,x_2,x_3,b_2,b_3)&=[\theta(b_2-b_3)I_0(M_{B_s}b_3\sqrt{x_1(1-x_2)})K_0(M_{B_s}b_2\sqrt{x_1(1-x_2)})+(b_2\leftrightarrow b_3)]\\&\times\begin{cases}K_0(M_{B_s}b_3\sqrt{x_1-x_3-x_1x_2+x_2x_3}), & x_1-x_3-x_1x_2+x_2x_3\geq0\\ \frac{i\pi}{2}H_0^{(1)}(M_{B_s}b_3\sqrt{|x_1-x_3-x_1x_2+x_2x_3|}), & x_1-x_3-x_1x_2+x_2x_3<0\end{cases}\end{aligned}\tag{A4}$$

$$h_e^1(x_2,x_3,b_2,b_3)=\frac{\pi i}{2}H_0^{(1)}(M_{B_s}b_2\sqrt{x_2x_3})\times[\theta(b_2-b_3)J_0(M_{B_s}b_3\sqrt{x_3})\frac{\pi i}{2}H_0^{(1)}(M_{B_s}b_2\sqrt{x_3})+(b_2\leftrightarrow b_3)],\tag{A5}$$

$$h_e^2(x_2,x_3,b_2,b_3)=\frac{\pi i}{2}H_0^{(1)}(M_{B_s}b_3\sqrt{x_2x_3})\times[\theta(b_2-b_3)J_0(M_{B_s}b_3\sqrt{x_2})\frac{\pi i}{2}H_0^{(1)}(M_{B_s}b_2\sqrt{x_2})+(b_2\leftrightarrow b_3)], \quad \text{(A6)}$$

$$\begin{aligned}h_g^1(x_1,x_2,x_3,b_1,b_2)=&[\theta(b_2-b_1)J_0(M_{B_s}b_1\sqrt{x_2x_3})\frac{\pi i}{2}H_0^{(1)}(M_{B_s}b_2\sqrt{x_2x_3})+(b_2\leftrightarrow b_1)]\\&\times\begin{cases}K_0(M_{B_s}b_1\sqrt{x_1x_2-x_2x_3}), & x_1x_2-x_2x_3\geq 0\\ \frac{i\pi}{2}H_0^{(1)}(M_{B_s}b_1\sqrt{|x_1x_2-x_2x_3|}), & x_1x_2-x_2x_3<0\end{cases}\end{aligned} \quad \text{(A7)}$$

$$\begin{aligned}h_g^2(x_1,x_2,x_3,b_1,b_2)=&[\theta(b_2-b_1)J_0(M_{B_s}b_1\sqrt{x_2x_3})\frac{\pi i}{2}H_0^{(1)}(M_{B_s}b_2\sqrt{x_2x_3})+(b_2\leftrightarrow b_1)]\\&\times\begin{cases}K_0(M_{B_s}b_1\sqrt{x_1+x_2+x_3-x_1x_2-x_2x_3}), & x_1+x_2+x_3-x_1x_2-x_2x_3\geq 0\\ \frac{i\pi}{2}H_0^{(1)}(M_{B_s}b_1\sqrt{|x_1+x_2+x_3-x_1x_2-x_2x_3|}), & x_1+x_2+x_3-x_1x_2-x_2x_3<0\end{cases}\end{aligned} \quad \text{(A8)}$$

where J_0 is the Bessel function and K_0, I_0 are modified Bessel function with $H_0^{(1)}(x)=J_0(x)+iY_0(x)$.

The evolution function $E(t_i)$ is defined by

$$\begin{aligned}E_{ef}(t_i)&=\alpha_s(t_i)\exp[-S_{B_s^0}(t_i)-S_{a_0^-}(t_i)],\\E_{af}(t_i)&=\alpha_s(t_i)\exp[-S_{a_0^+}(t_i)-S_{a_0^-}(t_i)],\\E_{nef}(t_i)&=\alpha_s(t_i)\exp[-S_{B_s}(t_i)-S_{a_0^+}(t_i)-S_{a_0^-}(t_i)]_{b_1=b_3},\\E_{naf}(t_i)&=\alpha_s(t_i)\exp[-S_{B_s}(t_i)-S_{a_0^+}(t_i)-S_{a_0^-}(t_i)]_{b_2=b_3}.\end{aligned} \quad \text{(A9)}$$

where the largest energy scales $t_i(i=a,c,e,g)$ to eliminate the large logarithmic radiative corrections are chosen as:

$$\begin{aligned}t_a^1&=\max\{M_{B_s}\sqrt{1-x_2},1/b_1,1/b_2\},\\t_a^2&=\max\{M_{B_s}\sqrt{x_1},1/b_1,1/b_2\},\\t_c^1&=\max\{M_{B_s}\sqrt{|x_1+x_2+x_3-x_1x_2-x_2x_3-1|},M_{B_s}\sqrt{x_1(1-x_2)},1/b_2,1/b_3\},\\t_c^2&=\max\{M_{B_s}\sqrt{|x_1-x_3-x_1x_2+x_2x_3|},M_{B_s}\sqrt{x_1(1-x_2)},1/b_2,1/b_3\},\\t_e^1&=\max\{M_{B_s}\sqrt{x_3},1/b_2,1/b_3\},\\t_e^2&=\max\{M_{B_s}\sqrt{x_2},1/b_2,1/b_3\},\\t_g^1&=\max\{M_{B_s}\sqrt{x_2x_3},M_{B_s}\sqrt{|x_1x_2-x_2x_3|},1/b_1,1/b_2\},\\t_g^2&=\max\{M_{B_s}\sqrt{x_2x_3},M_{B_s}\sqrt{|x_1+x_2+x_3-x_1x_2-x_2x_3|},1/b_1,1/b_2\}.\end{aligned} \quad \text{(A10)}$$

The $S_{B_s}(x_1)$, $S_S(x_i)$ used in the decay amplitudes are defined as:

$$\begin{aligned}S_{B_s}(x_1)&=s(x_1p_1^+,b_1)+\frac{5}{3}\int_{1/b_1}^t\frac{d\bar\mu}{\bar\mu}\gamma_q(\alpha_s(\bar\mu)),\\S_S(x_2)&=s(x_2p_2^+,b_2)+s(\bar x_2p_2^+,b_2)+2\int_{1/b_2}^t\frac{d\bar\mu}{\bar\mu}\gamma_q(\alpha_s(\bar\mu)),\\S_S(x_3)&=s(x_3p_3^-,b_3)+s(\bar x_3p_3^-,b_3)+2\int_{1/b_3}^t\frac{d\bar\mu}{\bar\mu}\gamma_q(\alpha_s(\bar\mu)),\end{aligned} \quad \text{(A11)}$$

where $\bar x_i=1-x_i$ and $\gamma_q=-\alpha_s/\pi$ is the anomalous dimension of the quark, and the Sudakov factor $s(Q,b)$ are resulting from the resummation of double logarithms and can be found in Ref. [44],

$$s(Q,b)=\int_{1/b}^Q\frac{d\mu}{\mu}\left[\ln\left(\frac{Q}{\mu}\right)A(\alpha(\bar\mu))+B(\alpha_s(\bar\mu))\right] \quad \text{(A12)}$$

with

$$A = C_F \frac{\alpha_s}{\pi} + \left[\frac{67}{9} - \frac{\pi^2}{3} - \frac{10}{27} n_f + \frac{3}{2}\beta_0 \ln\left(\frac{e^{\gamma_E}}{2}\right)\right] \left(\frac{\alpha_s}{\pi}\right)^2,$$
$$B = \frac{2}{3}\frac{\alpha_s}{\pi} \ln\left(\frac{e^{2\gamma_E - 1}}{2}\right), \tag{A13}$$

where γ_E and n_f are Euler constant and the active flavor number, respectively.

The threshold resummation factor $S_t(x)$ have been parametrized in [45], which is:

$$S_t(x) = \frac{2^{1+2c}\Gamma(\frac{3}{2}+c)}{\sqrt{\pi}\Gamma(1+c)} [x(1-x)]^c \tag{A14}$$

with the fitted parameter $c = 0.3$.

[1] K. Abe *et al.* (Belle Collaboration), Phys. Rev. D **65**, 092005 (2002).
[2] B. Aubert *et al.* (*BABAR* Collaboration), Phys. Rev. D **70**, 092001 (2004).
[3] N. N. Achasov and A. V. Kiselev, Phys. Rev. D **97**, 036015 (2018).
[4] D. Dou, X. Liu, J. W. Li, and Z. J. Xiao, J. Phys. G **43**, 045001 (2016).
[5] C. D. Lu, Y. M. Wang, and H. Zou, Phys. Rev. D **75**, 056001 (2007).
[6] P. Colangelo, F. De Fazio, and W. Wang, Phys. Rev. D **81**, 074001 (2010).
[7] W. Wang, Y. L. Shen, Y. Li, and C. D. Lu, Phys. Rev. D **74**, 114010 (2006).
[8] H. Y. Cheng, C. K. Chua, and K. C. Yang, Phys. Rev. D **73**, 014017 (2006).
[9] X. Liu and Z. J. Xiao, Phys. Rev. D **82**, 054029 (2010).
[10] Z. T. Zou, Y. Li, and X. Liu, Phys. Rev. D **97**, 053005 (2018).
[11] S. Cheng and J. M. Shen, Eur. Phys. J. C **80**, 554 (2020).
[12] X. Liu, Z. J. Xiao, and Z. T. Zou, Phys. Rev. D **88**, 094003 (2013).
[13] Q. X. Li, L. Yang, Z. T. Zou, Y. Li, and X. Liu, Eur. Phys. J. C **79**, 960 (2019).
[14] X. Liu, Z. J. Xiao, and Z. T. Zou, J. Phys. G **40**, 025002 (2013).
[15] H. Y. Cheng, C. K. Chua, and K. C. Yang, Phys. Rev. D **77**, 014034 (2008).
[16] M. G. Alford and R. L. Jaffe, Nucl. Phys. **B578**, 367 (2000).
[17] Y. L. Shen, W. Wang, J. Zhu, and C. D. Lu, Eur. Phys. J. C **50**, 877 (2007).
[18] J. D. Weinstein and N. Isgur, Phys. Rev. D **41**, 2236 (1990).
[19] M. Tanabashi *et al.* (Particle Data Group), Phys. Rev. D **98**, 030001 (2018).
[20] M. Ablikim *et al.* (BESIII Collaboration), Phys. Rev. Lett. **121**, 081802 (2018).
[21] M. Ablikim *et al.* (BESIII Collaboration), Phys. Rev. Lett. **121**, 022001 (2018).
[22] C. D. Lü, K. Ukai, and M. Z. Yang, Phys. Rev. D **63**, 074009 (2001).
[23] Y. Y. Keum, H. N. Li, and A. I. Sanda, Phys. Rev. D **63**, 054008 (2001).
[24] Y. Y. Keum, H. n. Li, and A. I. Sanda, Phys. Lett. B **504**, 6 (2001).
[25] A. Ali, G. Kramer, Y. Li, C. D. Lu, Y. L. Shen, W. Wang, and Y. M. Wang, Phys. Rev. D **76**, 074018 (2007).
[26] T. V. Brito, F. S. Navarra, M. Nielsen, and M. E. Bracco, Phys. Lett. B **608**, 69 (2005).
[27] K. Maltman, Phys. Lett. B **462**, 14 (1999).
[28] C. M. Shakin and H. Wang, Phys. Rev. D **63**, 074017 (2001).
[29] G. Buchalla, A. J. Buras, and M. E. Lautenbacher, Rev. Mod. Phys. **68**, 1125 (1996).
[30] H. n. Li and B. Tseng, Phys. Rev. D **57**, 443 (1998).
[31] H. Y. Cheng and K. C. Yang, Phys. Rev. D **71**, 054020 (2005).
[32] X. Liu, Z. T. Zou, Y. Li, and Z. J. Xiao, Phys. Rev. D **100**, 013006 (2019).
[33] Y. Li, C. D. Lu, Z. J. Xiao, and X. Q. Yu, Phys. Rev. D **70**, 034009 (2004).
[34] Z. J. Xiao, W. F. Wang, and Y. y. Fan, Phys. Rev. D **85**, 094003 (2012).
[35] T. Aaltonen *et al.* (CDF Collaboration), Phys. Rev. Lett. **108**, 211803 (2012).
[36] R. Aaij *et al.* (LHCb Collaboration), Phys. Rev. Lett. **118**, 081801 (2017).
[37] K. Nakamura *et al.* (Particle Data Group), J. Phys. G **37**, 075021 (2010).
[38] H. Y. Cheng, Phys. Rev. D **67**, 034024 (2003).
[39] A. V. Anisovich, V. V. Anisovich, and V. A. Nikonov, Eur. Phys. J. A **12**, 103 (2001).
[40] A. Gokalp, Y. Sarac, and O. Yilmaz, Phys. Lett. B **609**, 291 (2005).
[41] A. V. Anisovich, V. V. Anisovich, V. N. Markov, and N. A. Nikonov (SIGMA-AYAKS Collaboration), Phys. At. Nucl. **65**, 497 (2002).
[42] R. Aaij *et al.* (LHCb Collaboration), Phys. Rev. D **87**, 052001 (2013).
[43] T. M. Aliev and S. Bilmis, Eur. Phys. J. A **54**, 147 (2018).
[44] H. n. Li and K. Ukai, Phys. Lett. B **555**, 197 (2003).
[45] T. Kurimoto, H. n. Li, and A. I. Sanda, Phys. Rev. D **65**, 014007 (2001).